REVISTA INTERDISCIPLINAR DE PESQUISA EM ENGENHARIA

CILAMCE 2016
XXXVII IBERIAN LATIN AMERICAN CONGRESS ON COMPUTATIONAL METHODS IN ENGINEERING
BRASÍLIA - DF - BRAZIL

RESEARCH APPROACH OF MODELS USED IN MULTIAXIAL FATIGUE NUMERICAL SIMULATION

Jardel dos Santos Barbosa

jardelsbarbosa@gmail.com.br

Centro Universitário da FEI

Av. Humberto de Alencar Castelo Branco, 3972-B - Assunção, São Bernardo do Campo - SP, 09850-901, Brazil.

Debora Francisco Lalo

dflalo@fei.com.br

Centro Universitário da FEI

Av. Humberto de Alencar Castelo Branco, 3972-B - Assunção, São Bernardo do Campo - SP, 09850-901, Brazil.

William Manjud Maluf Filho

wmaluf@fei.edu.br

Centro Universitário da FEI

Av. Humberto de Alencar Castelo Branco, 3972-B - Assunção, São Bernardo do Campo - SP, 09850-901, Brazil.

Abstract. *During the operation of several equipments, there are lots of failure cases in mechanical components subjected to multiaxial stress, where among them stands out the fatigue phenomenon. In this context, this paper presents the failure mode as a life prediction model for multiaxial fatigue through numerical analysis using the finite element method, assessing in which situations, the equivalent stress-based models for static loads can also be used on estimating the multiaxial fatigue life with alternating loads. It will also be assessed the accuracy in which the approximation polynomial order of the element used for discretization has on the results.*

The literature review of this work addresses the definitions of stress states, alternating loads history, yield function models and later the life prediction for multiaxial fatigue. Given these definitions, the work focuses on performing a numerical simulation for a model submitted to

torsion and alternating tensile stresses. To validate the stress results obtained by computer simulation, experimental tests have been performed on prototypes by electrical extensometer. Then, using the signaled von Mises model, it will be discussed the influence that the used elements have on the multiaxial fatigue life results obtained through commercial software of multiphysics analysis Ansys®.

Keywords: *Finite element method, Multiaxial fatigue, Experimental data*

1 INTRODUCTION

Identifying possible failure modes of a mechanical component operation can ensure the safety and performance of a mechanical design. The ABNT 5462/94 standard defines mechanical failure as the total or partial reduction of working capacity of a part, component or machine to perform its function over a period, either because of a geometric change, or by fragmentation. A failure in one component is often undesirable for some reasons such as the risks to human life, environmental degradation, economic losses, damage to the image of companies and engineers. There are several causes for the occurrence of mechanical failures: corrosion, yielding of a material, fracture and fatigue (Collins, 2006). Therefore, the forecast is essential to not occur the process interruptions that generate high costs and customer dissatisfaction.

Unlike the various modes of mechanical failure, fatigue stands out as a phenomenon caused by the variation of the stress amplitude over the time. Usually, the fatigue failure occurs with stress intensity lower than the yielding limits of a material. In addition, the fracture can occur with low or no visible geometric plastic deformation, This feature makes it difficult to identify before the failure. (Callister and Rethwisch, 2002). Some statistics have demonstrated that the fatigue has a high number of occurrences. In a study performed in the United States by the National Bureau of Standards, currently called National of Institute Standarts and Tecnology (NIST), at 1983, with 230 components which showed mechanical failure, the fatigue was the cause of 61% of the cases, and also 65% of the occurrences were caused by design deficiencies as shown in Fig. 1 (Manson and Halford, 2006).

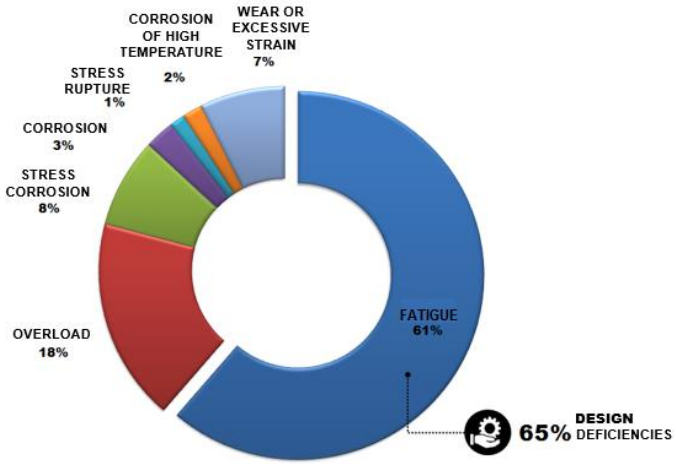

Figure 1. Failure modes in 230 components

The difficulty of obtaining a prediction about the failure of a mechanical component may occur also by limiting the analytical models have to predict stress states in geometries and complex loads. In this context, the numerical methods are highlighted, once they do not offer

exact responses of stress and strain such as the analytical methods, but instead they offer a wide range of applications, regardless of the structure geometry and loading condition (Alves Filho, 2007).

Fatigue analysis based on finite element method allows engineers and designers to predict the alternating multiaxial stress state with satisfactory speed and accuracy. The commercial softwares available help to identify critical points, however, they are limited to automate mathematical models, while knowledge of theories and performance of materials under cyclic stresses, necessary for predicting the durability and safety of mechanical components, are the responsibility of engineers and designers.

2 THEORETICAL BACKGROUND

2.1 Multiaxial states of stress

In general, the materials properties used in mechanical components are extracted from uniaxial tensile testing. However, in operating a component that is subjected to mechanical loads, the multiaxial stress state is produced according Fig. 2.

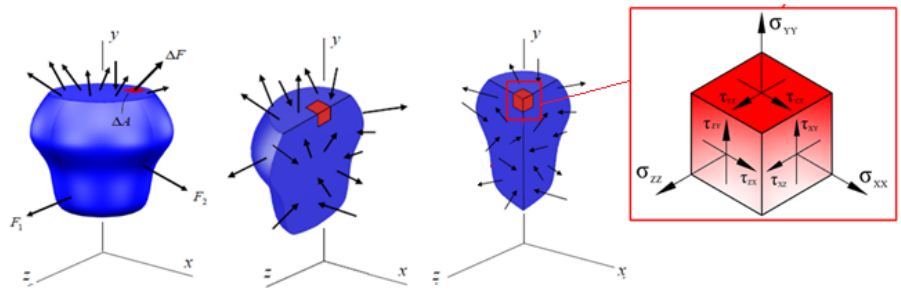

Figure 2. State stresses acting on an infinitesimal volume

The formulation of yield or failure criteria is formulated from the components of the multiaxial stress state in a material point. The symmetric Cauchy stress tensor in Eq. (1) representing the multiaxial stress state at a point has three components of normal stress to the coordinate axes and 6 shear components, accounting 9 components in total (Dieter, 1981).

$$T_{ij} = \begin{bmatrix} \sigma_{xx} & \tau_{xy} & \tau_{xz} \\ & \sigma_{yy} & \tau_{yz} \\ & & \sigma_{zz} \end{bmatrix} \tag{1}$$

One of the stress tensor properties is the existence of a set of orthogonal axes where the stress values are extreme, called principal stresses as indicated: σ_1, σ_2 e σ_3 (maximum, intermediate and minimum). These stresses are perpendicular to each other, thus forming a new coordinate system called principal coordinate system (Dieter, 1981). The three stress values are the roots of the cubic equation, according to Eq. (2) formed by eigen-values of the tensor T_{ij}, them these stresses have the characteristic of $\sigma_1 > \sigma_2 > \sigma_3$.

$$\sigma_p^{\,3} - I_1\sigma_p^{\,2} + I_2\sigma_p - I_3 = 0 \tag{2}$$

Where σ_p coefficients are stress tensor invariants, which keeps its steady value, even in a newly formed main coordinate system.

$$I_1 = \sigma_x + \sigma_y + \sigma_z \tag{3}$$

$$I_2 = \sigma_x\sigma_y + \sigma_y\sigma_z + \sigma_x\sigma_z - \tau_{xy}{}^2 - \tau_{yz}{}^2 - \tau_{xz}{}^2 \tag{4}$$

$$I_3 = \sigma_x\sigma_y\sigma_z + 2\tau_{xy}\tau_{yz}\tau_{xz} - \sigma_x\tau_{yz}{}^2 - \sigma_y\tau_{xz}{}^2 - \tau_{yz}{}^2 - \sigma_z\tau_{xy}{}^2 \tag{5}$$

Thus, the failure criteria are mathematical models for predicting the failure of a component subjected to a multiaxial stress state. They are applied in order to estimate a stress parameter which makes it possible the equivalence between multiaxial stress state and material strength data obtained from specimens subjected to uniaxial tension tests (Dieter, 1981).

2.1.1 The von Mises yield criterion

One of the most failure criteria used for the failure prediction of static loadings and multiaxial is the criterion of maximum octahedral shear stress, also known as von Mises criterion. It is based on the maximum shear stress acting at an oblique plane formed in the main coordinate system. This stress operates in a plane that intersects the three axes of the principal stresses at the same distance from the source. The stress used as an equivalent in comparison with the yield stress value is called von Mises equivalent stress expressed in relation to the tree-dimensional tensor components of stress and presented as Eq. (6):

$$\sigma_{VM} = \frac{1}{\sqrt{2}}\sqrt{(\sigma_X - \sigma_Y)^2 + (\sigma_Y - \sigma_Z)^2 + (\sigma_Z - \sigma_X)^2 + 6.(\tau^2{}_{xy} - \tau^2{}_{yz} - \tau^2{}_{xz})} \tag{6}$$

It may also be expressed in terms of principal stresses as Eq. (7):

$$\sigma_{VM} = \frac{1}{\sqrt{2}}\sqrt{(\sigma_1 - \sigma_2)^2 + (\sigma_2 - \sigma_3)^2 + (\sigma_3 - \sigma_1)^2} \tag{7}$$

Therefore, the failure occurs when the von Mises equivalent stress overcome the yielding limit obtained from a uniaxial tensile testing.

2.2 Finite element method

Most practical importance structures have complex geometry and loading which makes it difficult to calculate the stresses and displacements using the classical methods of analytical solid mechanics.

The Finite Element Method (FEM) is an approximate numerical technique used to obtain stresses and displacements into a structure.

The main action to be taken in the structural finite element analysis is to determine the relationship between the forces $\{F\}$ and the displacements fields $\{u\}$ of the entire structure as Eq. (8).

$$\{F\} = [K]\ \{u\} \tag{8}$$

The relation called by the stiffness $[K]$ is formed by the sum of the stiffness of each element used in the structure discretization.

For the three-dimensional elements the stiffness matrix is determined from the Eq. (9) for each element. Where the matrix $[B]$ is obtained from the shape functions partial derivatives in relation to the coordinate axes.

$$[K]_e = \int_V [B]^T [D][B] dV \tag{9}$$

Efficiency in the numerical treatment of the functions in FEM is influenced by the difficulty level of solving equations, due to the amount of discretizations created in the structure. Once this efficiency it is not always achieved just using the elements representation in the Cartesian system, the FEM uses the isoparametric formulation of the elements (Fig. 3). In this formulation, the displacement and geometry of each point element at the global cartesian system have an equivalence in the natural coordinate system (ξ, η, ζ). The displacement field within the element is given by functions called interpolation functions as in Eq. (10).

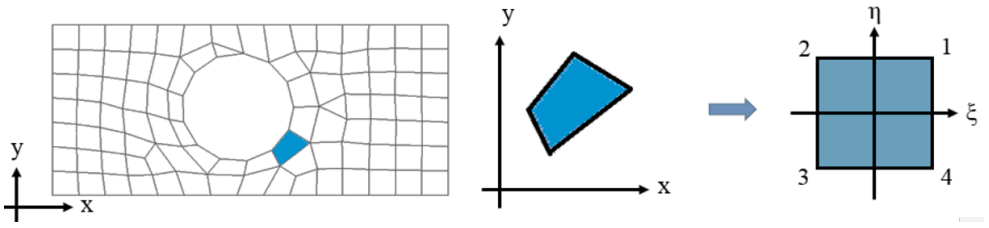

Figure 3. Isoparametric mapping

$$u(\xi,\eta,\zeta) = \sum_{i=1}^{q} N_i(\xi,\eta,\zeta) u_i \qquad v(\xi,\eta) = \sum_{i=1}^{q} N_i(\xi,\eta,\zeta) v_i \qquad w(\xi,\eta,\zeta) = \sum_{i=1}^{q} N_i(\xi,\eta,\zeta) w_i \tag{10}$$

The interpolation function determine the displacements inside the element, therefore, there is a numerical need to transform the derivatives from natural system (ξ, η, ζ) to the global system (x, y, z). According to Eq. (11) this coordinate transformation is accomplished by Jacobian operator [*J*].

$$\begin{Bmatrix} \frac{\partial N_i}{\partial x} \\ \frac{\partial N_i}{\partial y} \\ \frac{\partial N_i}{\partial z} \end{Bmatrix} = [J]^{-1} \begin{Bmatrix} \frac{\partial N_i}{\partial \xi} \\ \frac{\partial N_i}{\partial \eta} \\ \frac{\partial N_i}{\partial \zeta} \end{Bmatrix} \tag{11}$$

The determinant of the Jacobian operator is also the scale factor which relates the element volume calculated on the local system and the element volume of the global coordinate system. The stiffness matrix of the three-dimensional elements takes into account the volume calculation and the coordinate transformation from the natural element system to the global system, and can be written as shown in Eq. (12):

$$[K]_e = \int_{-1}^{1} \int_{-1}^{1} \int_{-1}^{1} [B]^T [D][B] \det[J] d\xi d\eta d\zeta \tag{12}$$

In general, commercial softwares use Gauss numerical integration for the solution of Eq. (12). This numerical integration technique utilizes the sum of a set of function values in a range of preselected points called Gauss points as in Fig. 4 and multiplied by a weight. The Gauss points are the sampling points used in the elements for calculating the numeric integration. These points are determined according to the geometry of the element.

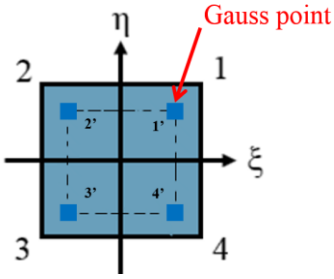

Figure 4. Gaussian points in a quadrilateral element

The stress components are extrapolated to the nearest node from the Gauss point of integration. The same node is simultaneously connected in more than one element, for this reason, the same node records stresses of several other points. The element mesh for a displacement field is continuous along the solid, however, the stress field is discontinuous as shown in Fig. 5a (Cook et al., 2002). To correct the discontinuity of the stress field surrounding the nodes, it is used the Eq. (13) to place the smoothed average of nodal values, where the average of the stress in Fig. 5b is obtained from each point of Gauss in order to minimize the global error.

$$\sigma_e^{ave} = \frac{1}{n}\sum_{i=1}^{n}(\sigma_e)_i \tag{13}$$

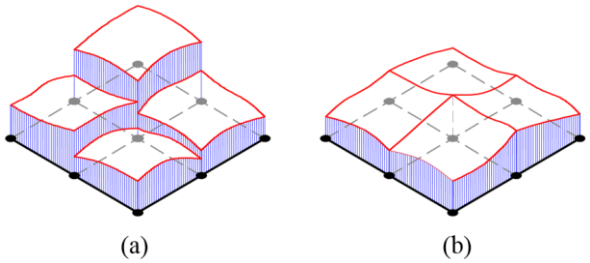

Figure 5. Discontinuity of the stresses of the element around the node: (a) unaverage (b) average

2.3 Fatigue

Most failures in mechanical components subjected to variable loads over time are due to fatigue. Fatigue is defined as a phenomenon that generates progressive and permanent located structural changes that occurs in materials subjected to cycles of stresses and deformations which may result in cracks or fracture after a sufficient number of cycles.

Generally three factors must occur simultaneously for the fatigue phenomenon occurs: cyclic loads, normal tensile and local plastic deformation. In some cases uniaxial prediction fatigue life criteria do not provide satisfactory results regarding the number of cycles that a component can resist. Thus, development is necessary to adjust the yielding criteria in order to obtain a number of cycles related to failure when it is submitted to a multiaxial stress state.

2.3.1 Cyclic history of loading

The use of a fatigue prediction model is influenced by the history of loading which the component is subjected. The cyclic history of loading identifies the stress amplitudes over time, which may be constant or variable. According to Fig. 6 is possible to see the diagrams indicating the variation of stress amplitude over time.

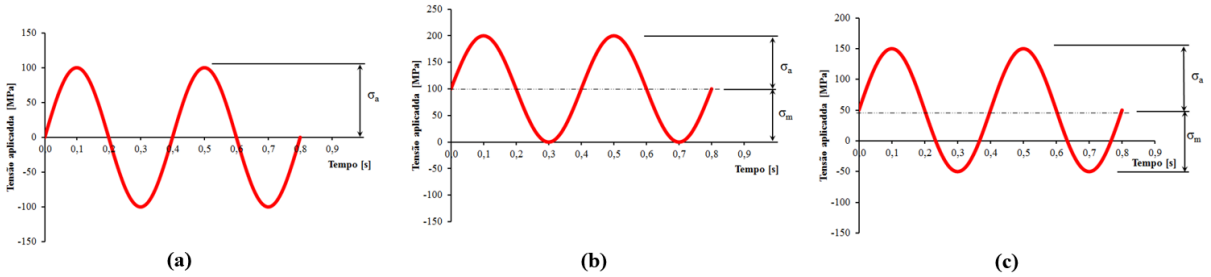

Figure 6. Sinusoidal cyclic loading: (a) R= -1 (b)R= 0 (c) -1 < R < 0.

Analyzing the load history is possible to extract three basic parameters for the use of predictive fatigue models: alternating stress amplitude σ_a, mean stress σ_m and stress amplitude ratio R.

$$\sigma_a = \frac{\sigma_{\max} - \sigma_{\min}}{2} \tag{14}$$

$$\sigma_m = \frac{\sigma_{\max} + \sigma_{\min}}{2} \tag{15}$$

$$R = \frac{\sigma_{mim}}{\sigma_{\max}} \tag{16}$$

The stress amplitude ratio may indicate whether or not the fatigue occurrence from the analysis of the loading history, for example: R=1 indicates static loading without the possibility of fatigue cracks nucleation. In its turn, the load history with 1 <R <∞ do not contribute to the phenomenon. The mechanical fatigue testing is applied to determine the behavior of materials under cyclic uniaxial loads and some engineering applications are made with sinusoidal history loadings as shown in Fig. 6a. A characteristic observed in a fully reversed constant loads (R=-1) is that the principal stress direction does not change over the loading history. This feature is plotted in Mohr's circle, showed in Fig.7 for plane stress.

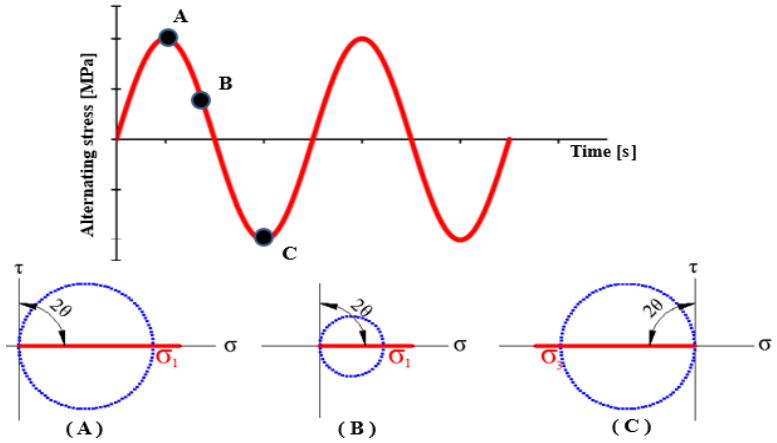

Figure 7. Direction of principal stress during cyclic loading for R= -1

Multiaxial fatigue is classified in two groups of load history: proportional loading and nonproportional loading, according to Fig. 8.

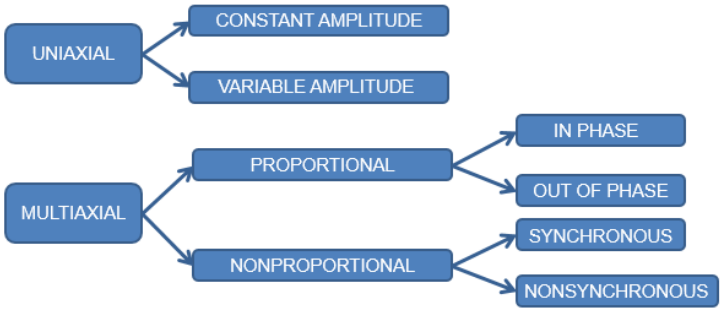

Figure 8. Fatigue loadings

When a multiaxial loading is classified as proportional, it refers to a history loading where the variation of the maximum and minimum amplitudes of stress remains fixed relating to the direction of the principal stresses axes (Meggiolaro and Castro, 2005). Proportional loading is divided into two types classified as in phase and out of phase (Marquis and Socie, 2000). Multiaxial loadings which reach the peaks of the maximum and minimum amplitude stress in the same instant throughout its history, according to Fig. 9, are classified as in phase (Marquis and Socie, 2000). Generally, loads in phase are always proportional.

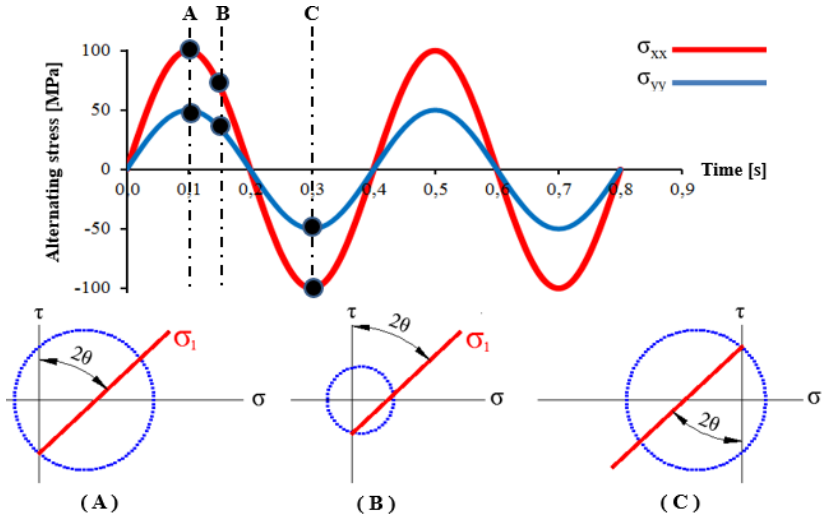

Figure 9. Proportional history loading in phase

On the other hand, historical loading where there is no such coincidence between the stress amplitude peaks are classified as out of phase, once there is a delay between periodic waves, and the lag angle variation can reduce the material fatigue life (Marquis and Socie, 2000).

2.4 Stress Based Models (*S-N* Curve)

The study and project methodologies for the fatigue life prediction follow three different approaches: stress-life cycles (*S-N*), strain-life cycles (ε-*N*) and fracture mechanics (*da/dN*) (Norton, 2013).

The S-N approach has been determined in a systematic way by August Wöhler determining the amplitude of the alternating stress S_a applied on a material until a number of cycles to failure occurs N_f. According to Eq. (17) S'_f and b are material constants obtained from the S-N curve showed in Fig. (10).

$$S_a = S'_f . (2N_f)^b \tag{17}$$

If the data of the high-cycle region of *S-N* curve are plotted in a log-log scale the format of the curve is a straight line (Dowling, 2000). Some materials present a baseline, called the fatigue limit *Sn*, so that alternating stress below this limit does not produce fatigue failure in the material. In general, this limit occurs for 1E6 loading cycles for ferrous materials.

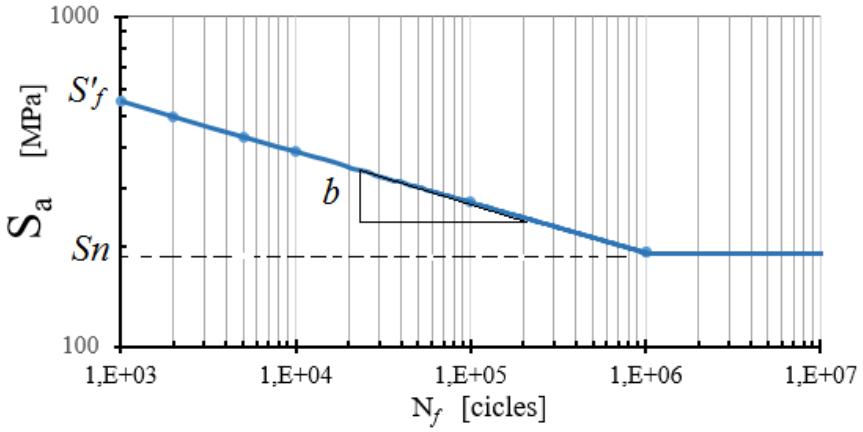

Figure 10. S-N diagram of material

The *S-N* curves are obtained for a material under very specific conditions, where in most cases they are not the same the conditions under which the component will operate, these differences decrease the fatigue strength of the material and should be corrected. The endurance fatigue limit for a N_f number of cycles in a component is corrected by the fatigue strength factor K_f. This factor considers the effects produced by the differences of size C_{size}, loading C_{load}, surface finish C_{surf}, temperature C_{temp} and reliability C_{reali} (Norton, 2013).

$$k_f = C_{size} C_{tload} C_{surf} C_{temp} C_{reali} \tag{18}$$

2.5 Mean stress correction

Several works show that the average stress influences negatively the number of cycles to failure, the higher its intensity the lower is the number of cycles. Thus, mathematical models seek to correct these effects on the *S-N* curve (Budynas and Nisbett, 2016). For a certain combination of σ_a and σ_m is determined equivalent completely reversed stress σ_{ar} which can be interpolated by the *S-N* curve obtained in a test with zero mean stress. One of the most used models is the Goodman correction model Eq. (19):

$$\sigma_{ar,Good} = \frac{\sigma_a}{1 - \frac{\sigma_m}{\sigma_{LR}}} \tag{19}$$

Thus, the cycles to failure prediction can be obtained by interpolating the *S-N* curve for replacing the S_a in Eq. (17) by the corrected σ_{ar} since the constants of material *S'f* and *b* are obtained in tests with zero mean stress. Dowling (2004) concludes in his paper that the Goodman model is excessive conservative for tensile mean stresses. Another model of mean stress correction is the Gerber expressed by Eq. (20):

$$\sigma_{ar,Gerb}=\frac{\sigma_a}{1-\left(\frac{\sigma_m}{\sigma_{LR}}\right)^2} \tag{20}$$

2.6 Multiaxial fatigue models

When a component is manufactured in a mechanical engineering material and it is subjected to an in phase and proportional loads history, it is possible to presume that the fatigue life is controlled by the amplitude of the octahedral shear stress and thus it uses the equations of von Mises model (Dowling, 1999).

Basically these models stipulate an equivalent stress to the multiaxial state of alternating stresses to which the body is subjected to use it as an input into the Eq. (17) and *S-N* curve of the material. One of the models used to estimate the fatigue life with proportional and in phase load history is based on the von Mises equivalent stress criterion. Where, it is formulated by using the alternating components of the stress tensor (Lee et al., 2011).

$$\sigma_{VM,a}=\frac{1}{\sqrt{2}}\sqrt{\left(\sigma_{X,a}-\sigma_{,aY}\right)^2+\left(\sigma_{Y,a}-\sigma_{Z,a}\right)^2+\left(\sigma_{Z,a}-\sigma_{X,a}\right)^2+6.(\tau^2{}_{xy,a}-\tau^2{}_{yz,a}-\tau^2{}_{xz,a})} \tag{21}$$

Equation (21) does not count the compressive stresses in the loading history, because the equivalent stresses values are always positive as shown in Fig.11.

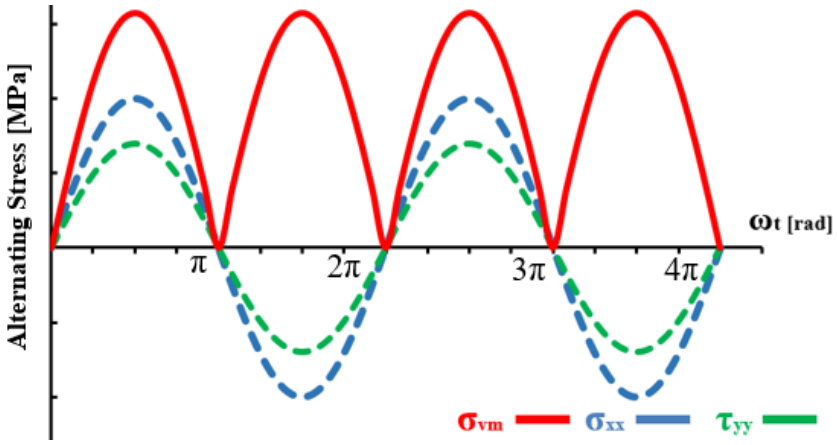

Figure 11. History loading using the von Mises stress

Therefore, the compression effects, which do not contribute to fatigue, are not taken into account. The signed von Mises stress can be used for considering these effects. This stress is obtained from a correction made in the Eq. (22) and this operation is done by inserting the maximum principal stress σ_1 signal if it is a nonzero value or in the case where the maximum principal stress σ_1 is zero, the operation can be done with the minimum principal stress σ_3.

$$\sigma_{VM,Signed}=\frac{\sigma_1}{|\sigma_1|}\left[\frac{1}{\sqrt{2}}\sqrt{\left(\sigma_1-\sigma_2\right)^2+\left(\sigma_2-\sigma_3\right)^2+\left(\sigma_3-\sigma_1\right)^2}\right] \tag{22}$$

The result of this correction can be seen according Fig. 12 in a sine wave format for the loading history.

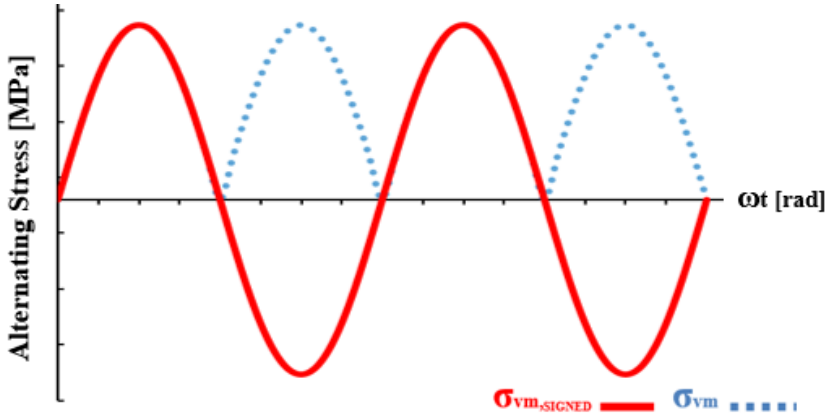

Figura 12. History loading using signed von Mises stress

The alternating amplitude stress showed in Eq. (14) can then be calculated with the maximum and minimum components of the signed von Mises stress. Another way to incorporate the von Mises stress in the alternating stress amplitude of the load history is by inserting positive or negative sign on the first invariant of the stress tensor I_1 calculated in Eq. (3) into a von Mises value obtained according Eq. (23) (Papuga et al., 2011).

$$\sigma_{a,VM} = \frac{Max\left|\sigma_{VM,a}\ \mathrm{sgn}(I_1)\right| - Min\left|\sigma_{VM,a}\ \mathrm{sgn}(I_1)\right|}{2} \tag{23}$$

The equivalent stress-based models are not efficient to describe the cyclic hardening of the material generated by a non-proportional cyclic loading. Therefore it is only recommended to use equivalent stress-based models to estimate the fatigue life of components that are subject to proportional and in phase loads (Lee et al., 2011).

3 NUMERICAL SIMULATION

It was considered four element types to determine the multiaxial stresses state and then it was applied the life prediction models. In this work, the static structural and fatigue analysis have been performed using the multiphysics analysis software Ansys.

3.1 Static structural analysis

The three-dimensional component simulated in Fig. 13 is a cantilever shaft fixed in one end and submitted to axial and torsional loads on the opposite side. The loads applied intend to produce a multiaxial state of shear and normal stresses in this study section.

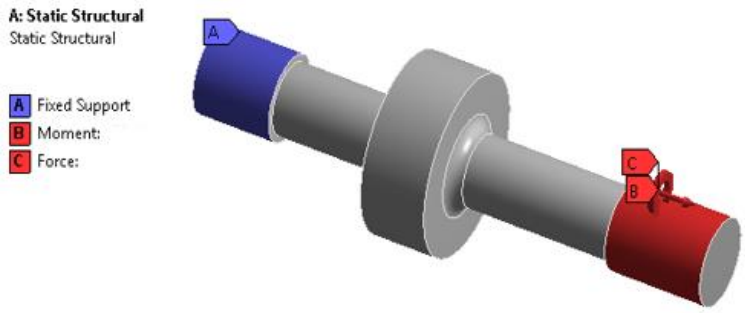

Figure 13. Geometry and boundary conditions of specimen

The shaft discretization was performed by using four element types such as tetrahedron (4 and 10-node) and hexahedron (8 and 20-node), formulated with interpolation functions of first and second order respectively. The number of nodes in each of the final four mesh elements is reported in Table 1.

Table 1. Number of nodes and elements in each simulation

Type of element	Nodes	Elements
TET4	4243	19954
HEX8	8280	7079
TET10	30183	20007
HEX20	31856	7079

By comparing the four types of mesh discretization in Fig. 14 it is possible to observe the influence that the higher order elements have on the component discretization. The TET12 and HEX20 elements are more accurate to discretize regions with complex geometry, once they are described by higher order interpolation functions.

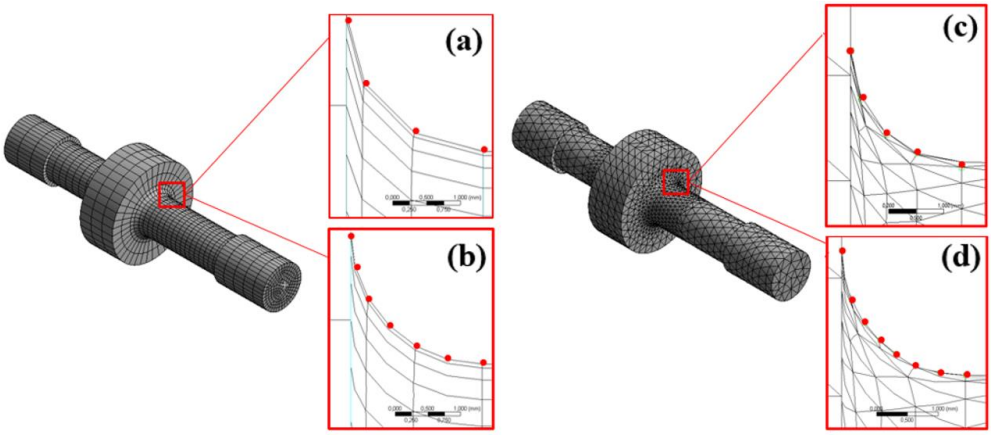

Figure 14. Complex geometry region discretized: (a) HEX8 (b)HEX20 (c)TET4 (d)TET10

Notched regions are stress concentrators and therefore there is a higher probability of having fatigue cracks nucleation. Another important factor in the finite element analysis is computational efforts to solve the equations. The higher the number of nodes in a mesh the higher the degrees of freedom, and consequently more accurate results will be obtained. However, the resolution time will increase. The mechanical properties in Table 2 were used in the simulation and have been based on the SAE 1045 steel.

Table 2. Mechanical material properties

Material	Young modulus (GPa)	Poisson ratio	Tensile yield strength (MPa)	Tensile ultimate strength (MPa)
SAE 1045	210	0.3	380	620

The intensity of axial and torsional loads is shown in Table 3.

Table 3. Simulation loads

Load	Magnitude
Moment	830 Nmm
Force	5500 N

Figure 15 shows the results from numerical simulation for static analysis.

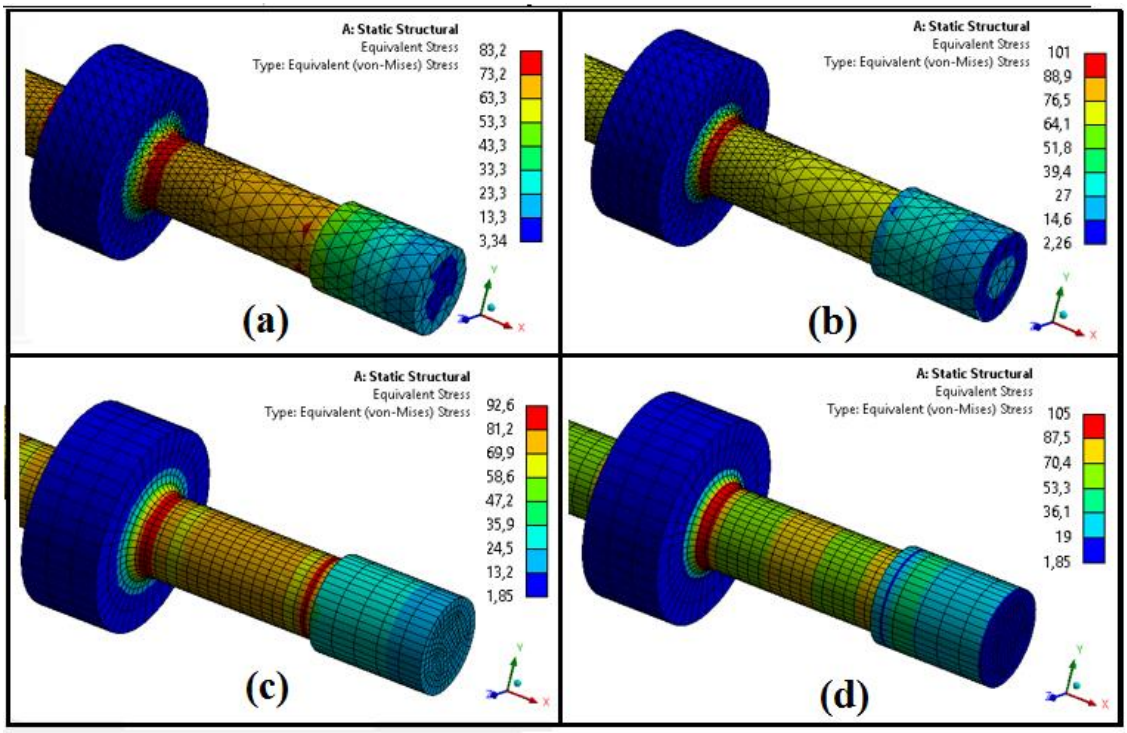

Figure 15. Results of von Mises stress in structural analysis for (a)TET4 (b)TET10 (c)HEX8 (d)HEX20

3.2 Experimental Data

To check the accuracy of the stress values obtained by the four finite element mesh in each analysis it was manufactured a Carbon steel SAE 1045 specimen with the same dimensions and loads used in numerical simulation. To simulate the loading conditions, it was manufactured a test device assembled on a torque machine as showed in Fig. 16. The device operates with a screw-thread system which allows the specimen to be submitted to two simultaneous loads of torsion and traction.

One of the specimen ends is kept fixed, hindering as rotating or displacement, the opposite end transmits the torque applied by a machine available on the Center of Mechanical Laboratories (CLM) in the University Center of FEI. The intensity of the applied torque can be measured by the load cell inside the torque machine, and visualized in data acquisition apparatus.

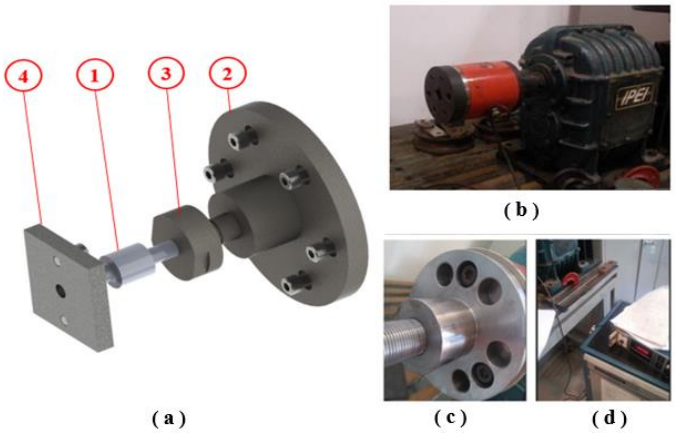

Figure 16. (a) Test device: (1) Specimen (2) Transmission plate (3) Tensile-torsional shaft (4) Cantilever plate (b) Torque machine (c) Fixing device on torque machine (d) Data acquisition of torque machine

The validation of the results obtained by the mesh was made using a strain gauge type rosette which allows measuring stresses in a two-dimensional state from the conversion of the variation in electrical resistance. Due to the dimensional limitations of the strain gauge in relation to the dimensional of specimen critical section, it was made the option to set the extensometer at a sampling point stress (Fig. 17) in a distance of approximately 8.5mm from the critical section obtained in the simulation.

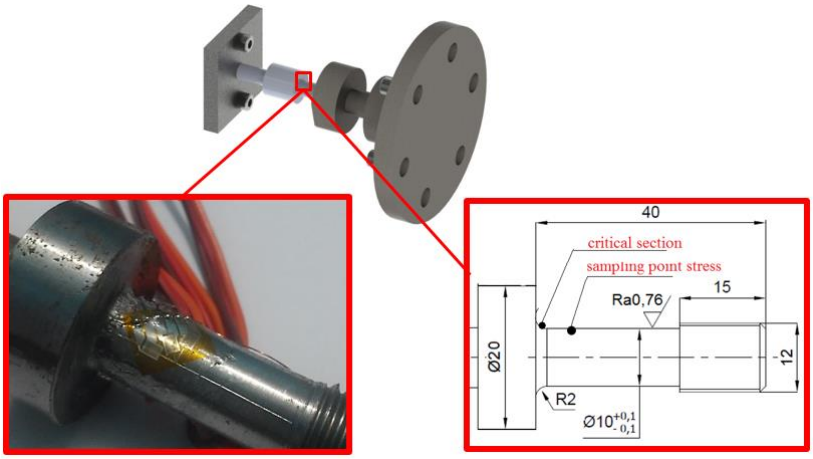

Figure 17. Details strain gauge Rosette in the sampling point

Considering the strain gauge components, the von Mises stress was calculated in the component surface obtained experimentally $\sigma_{VM,ex}$, and its intensity of stress was 79.21 MPa. The error between the von Mises stress obtained in the test $\sigma_{VM,ex}$ and von Mises stress obtained in the same point from the finite element analysis $\sigma_{VM,FEA}$ is presented in Table 4.

Table 4. Stress comparison on the sampling point data obtained in the test

Element	Node	$\sigma_{VM,FEA}$	Error
HEX20	7971	70,6	10,90%
HEX8	2469	70,4	11,10%
TET10	503	70,4	11,10%
TET4	503	70,2	11,40%

The critical section indicated in the static structural analysis can be estimated by the stress concentration factor $K_{T,Teo}$ available in the literature. Peterson (1951) provides curves where it is possible to estimate the $K_{T,Teo}$ value. Considering the geometry used in this paper the $K_{T,Teo}$ factor is approximately 1.6. A characteristic of the FEM is that the simulation already considers the influence of stress concentration factors. Then the geometry concentration factor used in the discretization can be estimated from the stresses. Table 5 shows the values obtained by $K_{T,FEA}$ for the different orders elements and the error compared to the $K_{T,Teo}$ estimated.

Table 5. *Kt* coefficient and error in critical section obtained in the simulation

Element	Node	$\sigma_{VM,FEA}$	$K_{T,FEA}$	Error
HEX20	7971	105	1.5	6.8%
HEX8	2469	92.6	1.3	18.0%
TET10	503	101	1.4	10.3%
TET4	503	83	1.2	26.1%

Analyzing the data from simulation and test it was observed that the second-order elements have a higher accuracy to discretize the complexity of the geometry and hence its obtained $K_{T,FEA}$ values are closer to the theoretical.

3.3 Experimental Fatigue Data

The cyclic material properties used in the fatigue simulations of this paper were those obtained from the work of Li et al., (2014) for a steel SAE1045. Values of S'_f and b coefficients used for building the S-N curve in the software have been calculated according to experimental data and they are presented in Table 6.

Table 6. Fatigue proprieties for the used material

Material	S'_f	b
SAE 1045	1763	-0.1527

3.4 Fatigue Analysis

To highlight the fatigue models in numerical simulation the loads intensity was increased as indicated in Table 7.

Table 7. Fatigue simulation loads

Load	Magnitude
Moment	2 kNmm
Force	12 kN

The multiaxial fatigue analysis was carried by using the higher stress components in the mesh. Table 8 shows the stress state for the four nodes of the critical section.

Table 8. Stress components of the nodes on the critical section

Element	Node	σ_1	σ_2	σ_3	σ_{vm}
HEX20	7971	258.7	56.0	-2.3	237,3
HEX8	2469	222.6	33.7	-3.4	209.9
TET10	503	255.1	54.8	4.5	229.6
TET4	503	206.2	46.4	27.9	169.8

The results of von Mises stress for the new load condition is shown in Fig. 18.

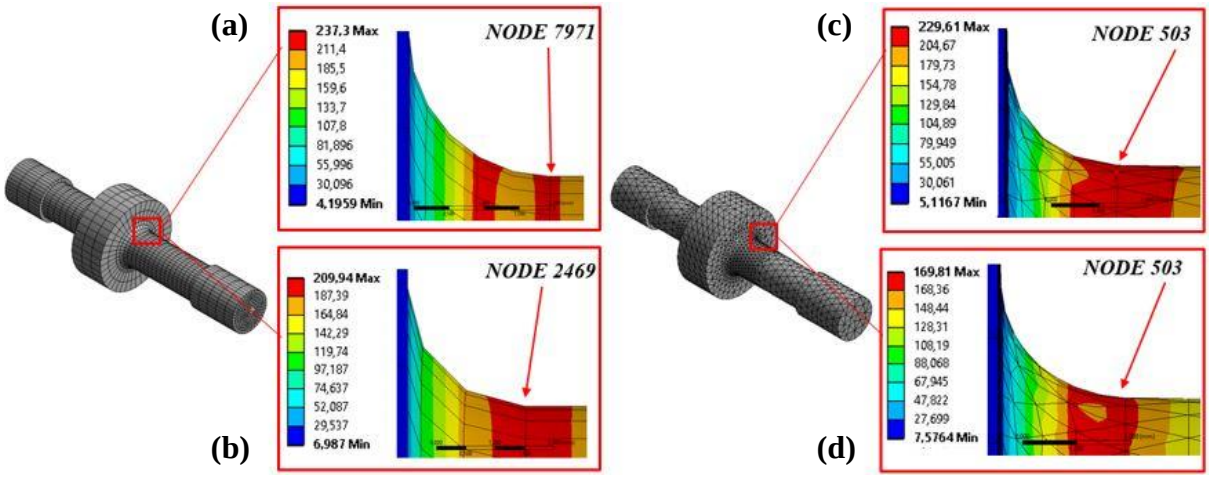

Figure 18. Maximum von Mises stress for fatigue analysis (a)HEX20 (b)HEX8 (c)TET10 (d)TET4

3.4.1 Multiaxial fatigue analysis with R = -1

The Stress-Life approach was applied to simulate a load history with *R*=-1 and the signed von Mises equivalent stress for interpolation in the log-log *S-N* curve. Three parameters that are available in the commercial software utilized for predicting life in multiaxial fatigue have been used: biaxiality indication *a*, equivalent alternating stress σ_{eas} and number of cycles N_f.

Multiaxial Fatigue criteria based on the signed von Mises equivalent stress, are only recommended for proportional loads history. Thus, the biaxiality indication *a* obtained by Eq. (24) and the angle ϕ_p in Fig. 19 can specify the nonproportionality generated by a loading. A loading is classified as proportional if *a* and ϕ_p remains constant along the time.

$$a = \frac{\sigma_2}{\sigma_1} \tag{24}$$

The range for biaxiality indicator goes from -1 up to 1. Once that zero indicates a state of uniaxial stresses and proportional loading, -1 indicates a state of pure shear and 1 corresponds to a biaxial state.

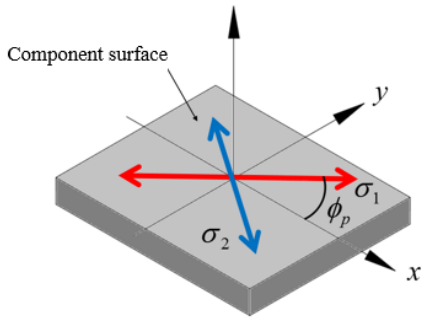

Figure 19. Surface stress reduced to two principal stresses and their orientation

The indication of biaxiality of the simulation is presented in Table 9.

Table 9. Biaxiality indicator

Element type	Node	Biaxiality indicator *a*
HEX8	2469	0,1514
HEX20	7971	0.2166
TET4	503	0.2250
TET10	503	0.2148

The range of values is positive and greater than zero, so as provided for simulation, the load is multiaxial and proportional. Therefore, equivalent alternating stress σ_{eas} can be calculated by using the signed von Mises stress as in Eq. (25).

$$\sigma_{eas} = \sigma_{a,VM} \cdot \frac{1}{Kf} \tag{25}$$

In this case, the mathematical operation of dividing the alternating stress by a fatigue strength factor K_f increases the intensity of the equivalent alternating stress. This operation is equal plotting a new S-N curve for the surface node analyzed in Fig. 20. The number of cycles until the fatigue failure is obtained by interpolating the equivalent alternating stress σ_{eas} at the S-N curve according to Eq. (26).

$$\sigma_{eas} = S'_f \cdot (2N_f)^b \tag{26}$$

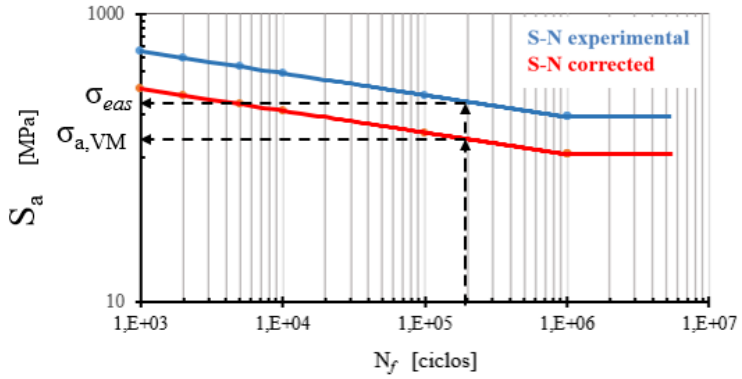

Figure 20. Interpolation log-log scale in S-N curve

The alternating stress amplitude, equivalent alternating stress and life prediction in simulation results are shown in Table 10 and Fig. 21.

Table 10. Alternating stress amplitude, equivalent alternating stress and life in simulation with R=-1

Element	Node	$\sigma_{a,VM}$	σ_{eas}	N_f
HEX20	7971	237.3	431.5	5042
HEX8	2469	209.9	381.7	11320
TET10	503	229.6	417.5	6268
TET4	503	169.8	308.6	45490

Reducing the order of the hexahedral elements from 20 to 8 nodes there was a decrease of about 12% in the equivalent alternating stress, but on the other hand the number of cycles was 55% higher.

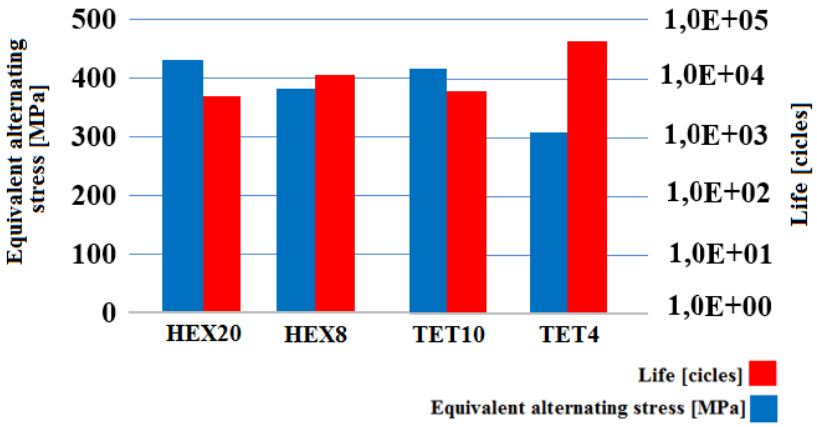

Figure 21. Comparative e between equivalent alternating stress and life in simulation with R=-1

By comparing the two second order elements HEX20 and TET10, the difference in the equivalent alternating stress was just 3%, but instead it generated a difference in number of cycles of 20%. This demonstrates how the number of cycles can be affected by small variations in stress caused by the reduction of the number of nodes and degrees of freedom of structure.

3.4.2 Multiaxial fatigue analysis with R = 0

In the fatigue case with *R=0*, it was researched how the effects of mean stress are used in the models available in the software. It was used the signed von Mises equivalent stress and the Goodman correction. The equivalent alternating stress used by software is given by Eq. (27). The use of this equation allows obtaining an equivalent stress value for different stress ratios *R*.

$$\sigma_{EAS,m} = \sigma_{a,VM} .C_m \frac{1}{Kf} \tag{27}$$

The results obtained by the Eq. (25) in the software simulation are equal to the equivalent completely reversed stress obtained through the Eq. (19) in Goodman model and Eq. (20) in Gerber model.

$$\sigma_{EAS,m} = \sigma_{ar}\frac{1}{Kf} = \sigma_{a,VM}.C_m\frac{1}{Kf} \tag{28}$$

The C_m is a constant for the mean stress correction of the Goodman model according to Eq. (29) and Gerber Model according to Eq. (30), *RR* is the stress ratio of the tests used to determine the S-N curve and σ_{LR} the ultimate tensile strength obtained from the uniaxial tensile test.

$$C_{m,Good} = \frac{\sigma_{LR}}{\sigma_{LR} - \sigma_m + \sigma_a\left(\frac{1+RR}{1-RR}\right)} \tag{29}$$

The C_m constant for the Gerber model in Eq. (30) does not use the components of the mean stress or alternating stress.

$$C_{m,Gerb} = \frac{(1-RR)^2.{\sigma_{LR}}^2}{2.Sn.(1+RR)^2}.\left(\sqrt{\frac{4.Sn.(1+RR)^2}{(1-RR)^2.{\sigma_{LR}}^2}} - 1\right) \tag{30}$$

Table 11 shows the respective values of the equivalent alternating stress using the Goodman and Gerber correction expressed by Eq. (27) in conjunction with the signed von Mises stress:

Table 11. Equivalent alternating stress and cycle number calculated by the equations

Element	Node	$\sigma_{ar,Good}$ Eq. (19)	$\sigma_{EAS,m}$ *Goodman corretion*	N*f* *Goodman corretion*	$\sigma_{ar,Gerb}$ Eq. (20)	$\sigma_{EAS,m}$ *Gerber corretion*	N*f* *Gerber corretion*
HEX20	7971	146.73	266.78	118100	123.16	223.93	371600
HEX8	2469	126.34	229.75	314110	108.05	196.48	862860
TET10	503	140.89	256.18	154010	118.88	216.15	468310
TET4	503	98.34	178.79	1000000	86.50	157.27	1000000

4 CONCLUSIONS

The analysis software for finite element proved to be an efficient tool for the characterization of multiaxial stress states that can cause fatigue failure and most of them include somehow tools for the fatigue analysis. Although the fatigue analysis is rather complex, there are different factors that may influence its life results accuracy, since the equivalent alternating stress interpolation in the *S-N* curve until the element order used in the numerical simulation. The models based on the equivalent stress to static loads have a restricted use when applied in fatigue analysis, and then the von Mises model should be applied only in situations of proportional and in-phase loading history.

In the fatigue analysis performed by the software the equivalent alternating stress used to interpolate the number of cycles in the S-N curve was corrected by a factor called fatigue strength factor K_f. In this single coefficient, the software does all the considerations regarding

the differences between the fatigue resistance obtained from the specimen under ideal conditions and simulated component. In some cases mechanical components with high stress concentrator geometries and different surface finishes can be a source of error if the appropriate corrections are not considered.

The equivalent stress-based models results are greatly influenced by the accuracy of the element mapping to be considered. The most complete second order element HEX 20 has proved to be the most accurate when discretize the critical section. Furthermore, it also proved to be the element that can estimate the most conservative and favourable safety fatigue life results. The first order elements can be an alternative to reduce the number of equations to be solved, however it can produce a large increase in the number of cycles and thus a source of error in predicting life. This happens because the number of cycles depends on the von Mises equivalent stress data for a logarithmic interpolation of the *S-N* curve.

5 REFERENCES

Alves Filho, A., 2006. Elementos Finitos - a Base da Tecnologia Cae. Érica

Callister, W.D.; Rethwisch, D.G. 2012. Ciência e Engenharia de Materiais. 8. ed. Grupon Gen

Collins, J. A. 2006. Projeto mecânico de elementos de máquinas: uma perspectiva de prevenção da falha. LTC

Cook, R., Maltus, D., Plesha, M., Witt, R., 2002. Concepts and Applications of Finite Element Analysis. Wiley

Dieter, G.E., 1981. Metalurgia Mecânica. Guanabara Dois

Dowling N.E, 1999. Mechanical Behavior of Materials. 2. ed. Prentice Hall

Dowling, N.E, 2004. Mean Stress Effects in Stress-Life and Strain-Life Fatigue. Society of Automotive Engineers

Lee, Y. L., Barkey, M. E., Kang, H. -T.,2011. Metal Fatigue Analysis Handbook: Practical Problem Solving Techniques for CAE. Butterworth-Heinemann

Li, B. C. Jiang C.; Han X.; Li Y. 2014. A new approach of fatigue life prediction for metallic materials under multiaxial loading. International Journal of Fatigue

Marquis, G.; Socie, D. F., 2000. Multiaxial Fatigue. Society Of Automotive Engineers (SAE)

Meggiolaro, M.; Castro, J. T. P. D., 2005. Comparação entre métodos de previsão de vida à fadiga sob cargas multixiais I. 60º Congresso Associação Brasileira de Metalurgia e Materiais ABM

Norton, R.L., 2013. Projeto de Máquinas - Uma Abordagem Integrada. Bookman

Budynas R. G.; Nisbett J. K., 2016. Elementos de Máquinas de Shigley. McGraw-Hill.

Papuga, J.; Vargas, M.; Hronek, M., 2000. Evaluation of uniaxial fatigue criteria applied to miltiaxially loaded unntched samples. Engineering MECHANICS, v. 19, p. 99-111

Peterson, R.E, 1951. Design factors for stress concentration. Machine design